Electronic Supplementary Information

Label-free and enzyme-free detection of microRNA based on hybridization chain reaction with hemin/G-quadruplex enzymatic catalysis-induced MoS_2 quantum dots inner filter effect

Jia Ge, [*a] Zhangyu Qi,[b] Liangliang Zhang,[b] Xueping Shen,[a] Yanmei Shen,[a] Weixia Wang,[a] Zhaohui Li [a]

[a] College of Chemistry, Green Catalysis Center, Zhengzhou University, Zhengzhou, 450001, P. R. China; E-mail address: jiage@zzu.edu.cn.

[b] State Key Laboratory for the Chemistry and Molecular Engineering of Medicinal Resources, School of Chemistry and Pharmaceutical Sciences, Guangxi Normal University, Guilin, 541004, P. R. China.

Materials

The oligonucleotides used were synthesized by Shanghai Sangon Biological Engineering Technology & Services Co.,Ltd. The sequences of the DNA oligonucleotides were as follows:

let-7a: 5′-UGA GGU AGU AGG UUG UAU AGUU-3′;

let-7b: 5′- UGA GGU AGU AGG UUG UGU GGUU-3′;

let-7f: 5′- UGA GGU AGU AGA UUG UAU AGUU-3′;

let-7g: 5′- UGA GGU AGU AGU UUG UAC AGUU-3′;

miR-21: 5′-UAG CUU AUC AGA CUG AUG UUGA-3′;

miR-141: 5′-UAA CAC UGU CUG GUA AAG AUGG-3′;

HP1: 5′-AGG GCG GGT GGG TTG TAT AGT AGG CAA AGT AAC TAT ACA ACC TAC TAC CTC ATG GGT-3′

HP2: 5′-TGG GTA CTT TGC CTA CTA TAC AAT GAG GTA GTA GGT TGT ATA GTA GGG TAG GGC GGG-3′

HP3: 5′-TGGG TTG TAT AGT AGG CAA AGT AAC TAT ACA ACC TAC TAC CTC ATG GGT-3′

HP4: 5′-TGG GTA CTT TGC CTA CTA TAC AAT GAG GTA GTA GGT TGT ATA GTA-3′

Sodium molybdate dihydrate ($Na_2MoO_4 \cdot 2H_2O$) was purchased from J&K Chemical (Beijing, China). Glutathione (GSH), hemin, 30% hydrogen peroxide (H_2O_2) and o-phenylenediamine (OPD) were obtained from Sinopharm Chemical Reagent Co., Ltd. (Shanghai, China). Diethylprocarbonate (DEPC)-treated deionized water

and hemin were purchased from Shanghai Sangon Biotechnology Co., Ltd. (Shanghai, China). All other reagents were used as received without further purification. DEPC-treated deionized water was used in all experiments.

Instruments

Transmission electron microscopy images (TEM) were obtained by transmission electron microscope (JEOL Model JEM-2010F) at an accelerating voltage of 200 kV. Atomic force microscopy (AFM) images were obtained on Multimode Nano-scope V scanning probe microscopy (Bruker, Germany). X-ray photoelectron spectroscopy (XPS) measurements were recorded on an ESCALAB 250Xi (Thermo Scientific, America). UV-visible (UV-vis) absorption spectra were taken using a Cary Bio-100 UV/Vis spectrometer (Varian). Fluorescence life time was carried on FLS 980 fluorometer (Edinburgh Instrumentds Ltd.) The fluorescence measurements were carried out on a FL-4600 spectrophotometer (Hitachi, Japan). The fluorescence emission spectra were collected from 330 nm to 630 nm at room temperature with a 318 nm excitation wavelength.

Real sample assay

In order to prove the viability of our proposed sensors for practical applications, human serum was adopted as a model matrix. Human serum samples were treated by centrifugation at 10,000 rpm for 10 min. Next, the supernatant was diluted by ultrapure so that original miRNA concentration could fall in the standard calibration curve of this assay. The supernatant was spiked with additional known concentrations of miRNA (1, 5, and 10 pM). The detection procedure was the same as that described in the aforementioned experiment for miRNA detection in buffer. The serum from

volunteers was collected by the First Affiliated Hospital of Zhengzhou University, and informed consent was obtained. All experiments were performed in compliance with the relevant laws and institutional guidelines and approved by the Life Science Ethics Review Committee of Zhengzhou University.

Table S1. Comparison of different methods for the determination of miRNA.

Mode	Amplification strategy	Target	LOD	Ref.
Electrochemistry	Pt/Sn−In_2O_3 nanoflower	miR-21	1.92 fM	1
Electrochemistry	biotinylated polythiophene films	miR-221	0.7 pM	2
Electrochemistry	WS_2 nanosheet	miR-21	180 pM	3
SERS	metal-dielectric nanostructures	miR-222	485 pM	4
Fluorescence	AuNP based hairpin-locked-DNAzyme probe	miR-141	25 pM	5
Fluorescence	WS_2 nanosheet and duplex-specific nuclease	miR-21	300 fM	6
Fluorescence	near-infrared Ag_2S quantum dots	miR-20a	12 fM	7
Fluorescence	molecular beacons and duplex-specific nuclease	let-7a	0.4 pM	8
Fluorescence	graphene quantum dots	miR-155	100 pM	9
Fluorescence	graphene	let-7a	14.7 nM	10
Colorimetry	gold nanoparticles and duplex-specific nuclease	miR-122	16 pM	11
Fluorescence	MoS_2 quantum dots and hybridization chain reaction	let-7a	42 fM	This work

Fig. S1. The XRD spectrum of MoS_2 quantum dots

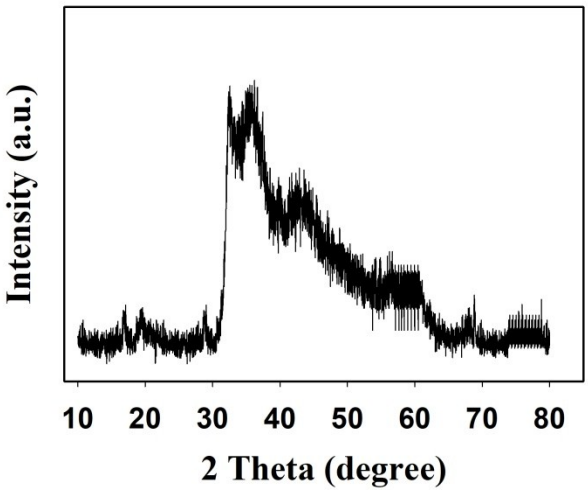

Fig. S2. The EDS spectrum of MoS_2 quantum dots

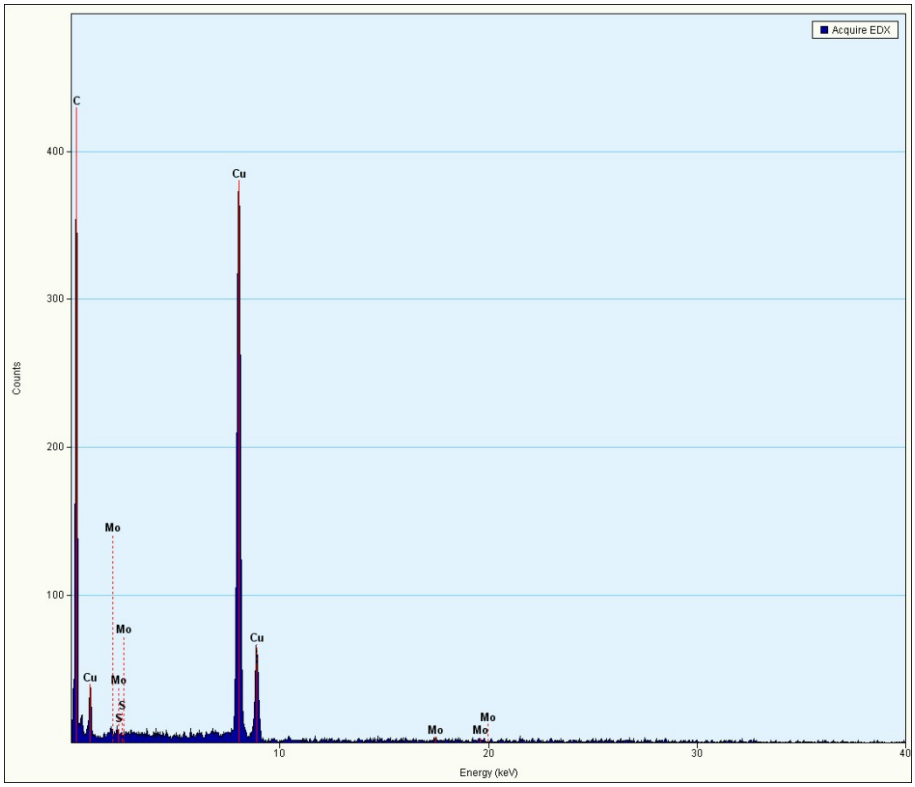

Fig. S3. Fluorescence intensity variation of MoS_2 quantum dots at various concentrations of NaCl.

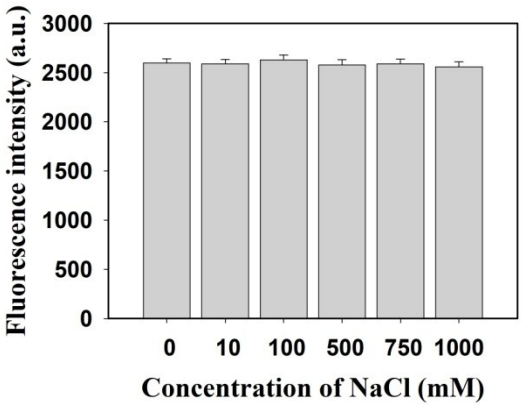

Fig. S4. Effects of UV irradiation time on the fluorescence intensity variation of the MoS_2 quantum dots.

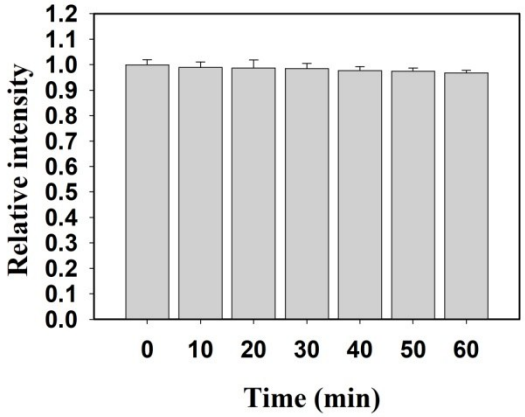

Fig. S5. Fluorescence decay curves of MoS_2 quantum dots in the absence and presence of DAP.

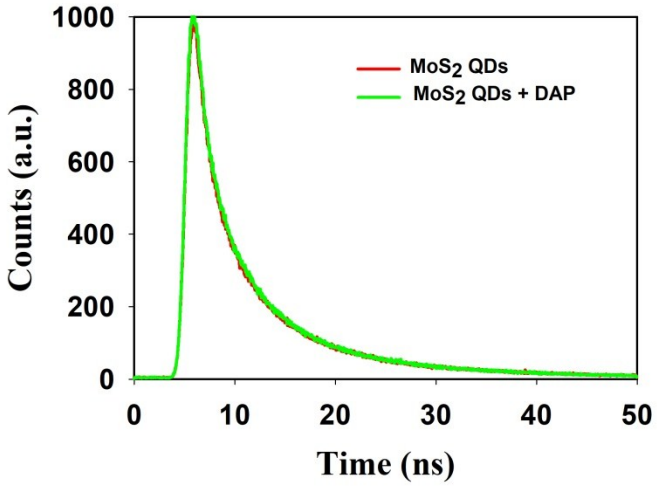

Fig. S6. Agarose gel electrophoresis image of HCR products. Lane 1: HP1; Lane 2: HP1 + HP2; Lane 3: HP1 + HP2 + miRNA let-7a; Lane M is the DNA size marker.

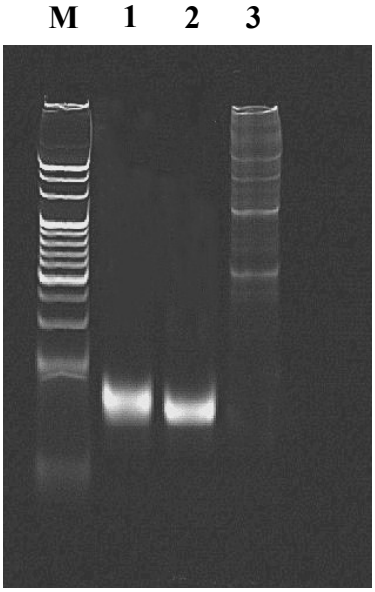

Fig. S7. (A) The fluorescence of MoS_2 quantum dots in the absence (curve a) and presence of hemin (curve b: 2 μM; curve c: 20 μM); (B) Effect of the concentrations of hemin on MoS_2 quantum dots.

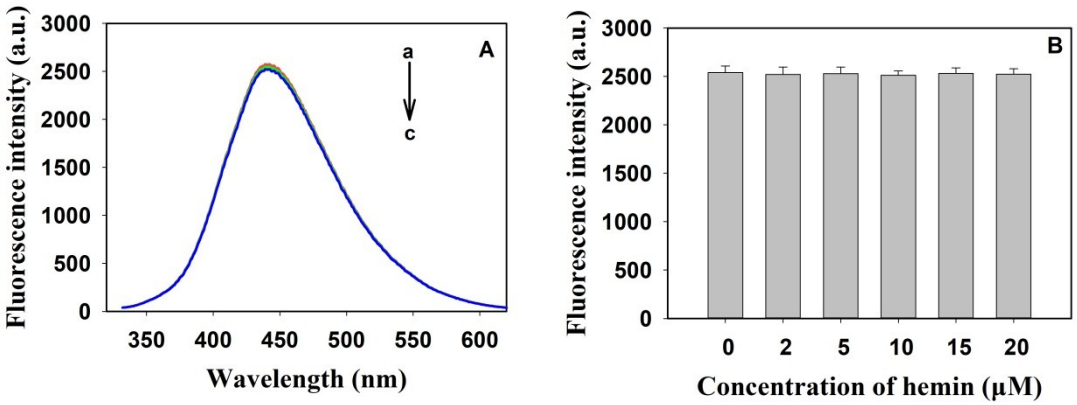

Fig. S8. (A) The fluorescence of MoS_2 quantum dots in the absence (curve a) and presence of H_2O_2 (curve b: 2 mM; curve c: 20 mM); (B) Effect of the concentrations of H_2O_2 on MoS_2 quantum dots.

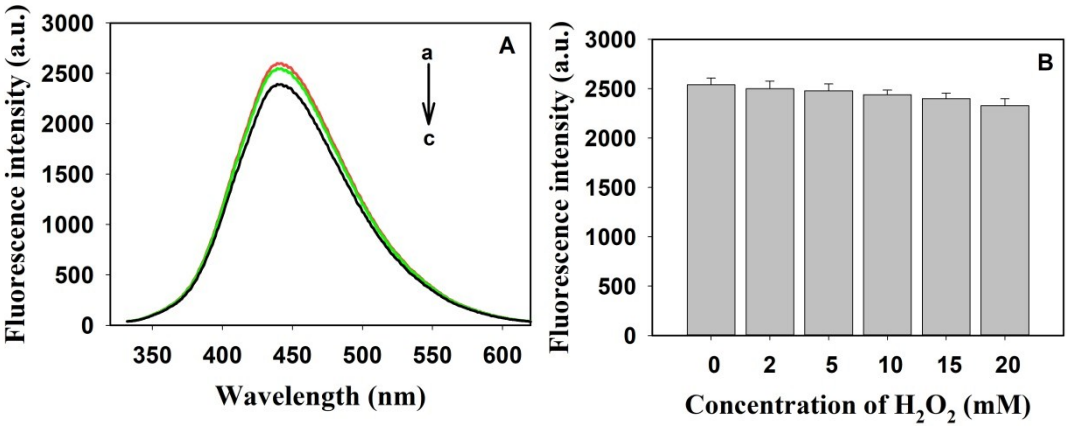

Fig. S9. Effect of reaction time on the sensing system.

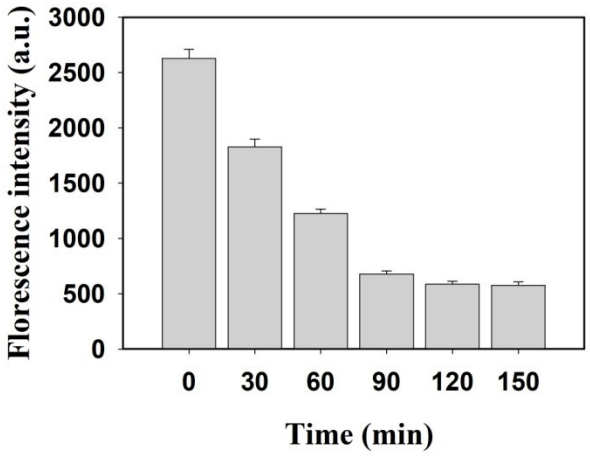

Fig. S10. Effect of the concentrations of hemin on the sensing system.

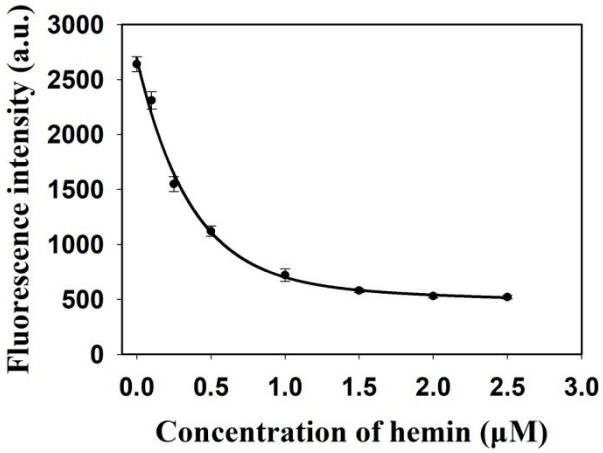

Fig. S11. Effect of the concentrations of OPD on the sensing system.

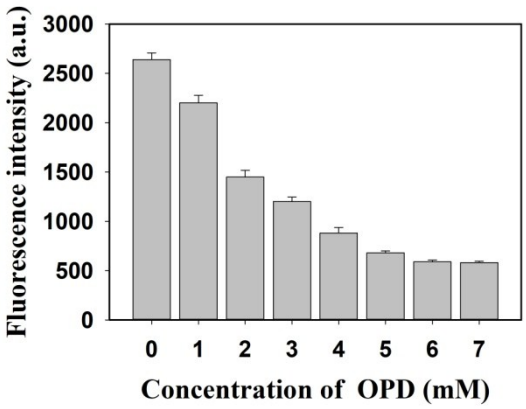

Fig. S12. Effect of the concentrations of H_2O_2 on the sensing system.

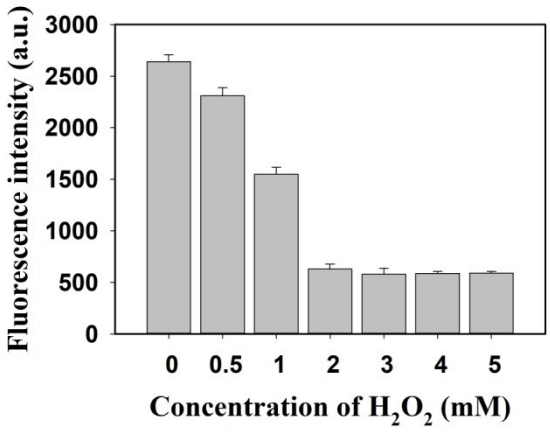

Fig. S13. (A) Mean diameters and (B) fluorescence intensity of MoS_2 quantum dots after incubation in human serum.

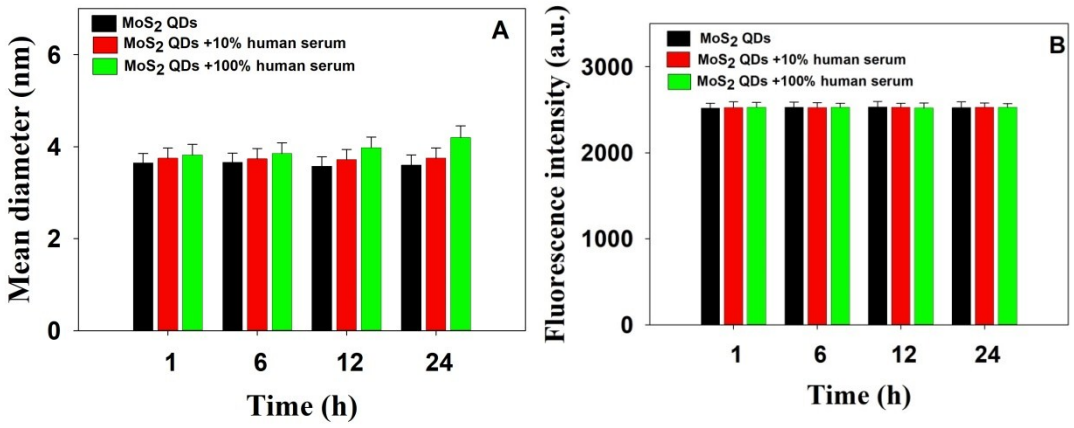

References

1 K. Zhang, H. F. Dong, W. H. Dai, X. D. Meng, H. T. Lu, T. T. Wu, and X. J. Zhang, *Anal. Chem.*, 2017, **89**, 648-655.

2 D. Voccia, M. Sosnowska, F. Bettazzi, G. Roscigno, E. Fratini, V. De Franciscis, G. Condorelli, R. Chitta, F. D'Souza, W. Kutner and I. Palchetti, *Biosens. Bioelectron*., 2017, **87**, 1012-1019.

3 J. J. Zhao, X. Jin, M. Vdovenko, L. L. Zhang, I. Y. Sakharov, and S. L. Zhao, *Chem. Commun.*, 2015, **51**, 11092-11095.

4 A. Chiadò, C. Novara, A. Lamberti, F. Geobaldo, F. Giorgis, and P. Rivolo, *Anal. Chem.*, 2016, **88**, 9554-9563.

5 Y. J. Yang, J. Huang, X. H. Yang, X. X. He, K. Quan, N. L. Xie, M. Ou, and K. M. Wang, *Anal. Chem*., 2017, **89**, 5850-5856.

6 Q. Xi, D. M. Zhou, Y. Y. Kan, J. Ge, Z. K. Wu, R. Q. Yu, and J. H. Jiang, *Anal. Chem.*, 2014, **86**, 1361-1365.

7 P. Miao, Y. G. Tang, B. D. Wang, and F. Y. Meng, *Anal. Chem.*, 2016, **88**, 7567-7573.

8 X. Y. Lin, C. Zhang, Y. S. Huang, Z. Zhu, X. Chen, and C. J. Yang, *Chem. Commun*., 2013, **49**, 7243-7245.

9 H. Hang, Y. S. Wang, D. W. Zhao, D. D. Zeng, J. Y. Xia, A. Aldalbahi, C. G. Wang, L. L. San, C. H. Fan, X. L. Zuo, and X. Q. Mi, *ACS Appl. Mater. Interfaces*, 2015, **7**, 16152-16156.

10 H. Y. Liu, L. Li, Q. Wang, L. L. Duan, and B. Tang, *Anal. Chem*., 2014, **86**,

5487-5493.

11 Q. Wang, R. D. Li, B. C. Yin, and B. C. Ye, *Analyst*, 2015, **140**, 6306-6312.